THE JOURNAL OF PHYSICAL CHEMISTRY B

ARTICLE

pubs.acs.org/JPCB

Comprehensive Solid-State NMR Analysis Reveals the Effects of N-Methylation on the Molecular Dynamics of Glycine

Jing Huang,[†,‡] Limiao Jiang,[†,‡] Pingping Ren,[†,‡] Limin Zhang,[†] and Huiru Tang*[,†]

[†]State Key Laboratory of Magnetic Resonance and Atomic and Molecular Physics, Wuhan Institute of Physics and Mathematics, Wuhan 430071, P.R. China

[‡]Graduate School of Chinese Academy of Sciences, Beijing 100049, P.R. China

Supporting Information

ABSTRACT: Molecular dynamics of metabolites are important for their interactions and functions. To understand the structural dependence of molecular dynamics for N-methylated glycines, we comprehensively measured the ^{13}C and ^{1}H spin−lattice relaxation times for sarcosine, *N*,*N*-dimethylglycine, betaine, and betaine hydrochloride over a temperature range of 178−460 K. We found that the reorientations of methyl groups were observed for all these molecules, whereas reorientations of whole trimethylamine groups were detected in betaines. While similar rotational properties were observed for methyl groups in *N*,*N*-dimethylglycine and those in betaine, three methyl groups in betaine hydrochloride had different motional properties ($E_a \approx 20.5$ kJ/mol, $\tau_0 \approx 1.85 \times 10^{-13}$ s; $E_a \approx 13.9$ kJ/mol, $\tau_0 \approx 2.1 \times 10^{-12}$ s; $E_a \approx 15.8$ kJ/mol, $\tau_0 \approx 1.1 \times 10^{-12}$ s). *N*,*N*-Dimethylglycine showed a phase transition at 348.5 K with changed relaxation behavior for methyl groups showing distinct E_a and τ_0 values. The DIPSHIFT experiments showed that CH_3 and CH_2 moieties in these molecules had dipolar-dephasing curves similar to these moieties in alanine and glycine. The activation energies for CH_3 rotations positively correlated with the number of substituted methyl groups. These findings provided useful information for the structural dependence of molecular dynamics for N-methylated glycines and demonstrated solid-state NMR as a useful tool for probing the structure−dynamics relationships.

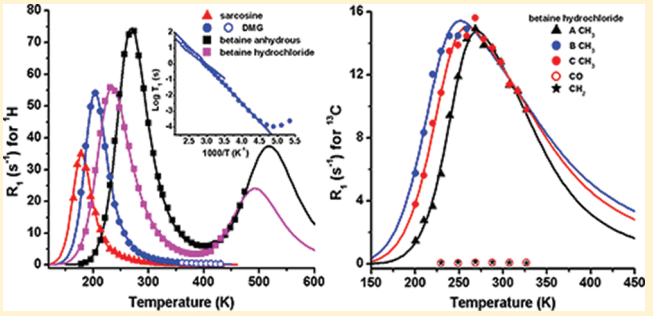

1. INTRODUCTION

The relationship between molecular structure and properties is an important topic for both fundamental and applied researches especially for biopolymers and pharmaceuticals. It is well-known that molecular dynamics of drugs are closely related to their polymorphic properties which in turn affect physical, pharmacological, and stability properties of these pharmaceuticals.[1,2] Molecular dynamics of biopolymers are probably associated with their physical and mechanical properties, such as phase and rheological behaviors, as well as the functional properties of biopolymers such as proteins and polysaccharides. However, the structural dependence of molecular dynamics remains to be fully understood although such dependence is deemed essential. To approach this complex issue, a well designed series of simple molecules with a distribution of structural properties is required as a good starting model system. The combined physical methods such as DSC, X-ray diffraction, and solid state NMR represent some powerful investigative tools.

Solid state NMR is an effective technique to approach the aforementioned complex problem since measurements of NMR relaxation times and dipolar interactions can facilitate the access of the molecular dynamic information in multiple time scales. For example, the measurements of proton spin−lattice relaxation times (T_1, $T_{1\rho}$) enable the detection of molecular motions in nano- and microseconds whereas the dipolar interaction measurements with techniques such as DISHIFT[3] can probe motions occurring above the tens of kiloherz frequency scale; slow motions (milliseconds to seconds) can be detected with so-called exchange NMR experiments.[4,5] In fact, the combination of these solid state NMR techniques have already found widespread successful applications in studies of the molecular motions of amino acids and proteins,[6−9] complex plant polysaccharides[10−12] and their structural units,[13,14] and other biopolymers[15−17] over a range of motional frequencies.

N-Methylated glycines including *N*-methylglycine (sarcosine), *N*,*N*-dimethylglycine (DMG), *N*,*N*,*N*-trimethylglycine (betaine), and *N*,*N*,*N*-trimethylglycine hydrochloride (betaine hydrochloride) represent a good sets of samples for understanding the effects of N-methylation on the dynamics of resultant glycine derivatives. These molecules are interconvertible metabolites in animals, plants, and microorganisms with various functions. For example, betaine is an important osmolyte being able to affect the

Received: October 31, 2011
Revised: December 2, 2011
Published: December 05, 2011

structural properties of proteins and nucleic acids.[18,19] It is also a vital cofactor in methylation cycle which donates methyl groups in biosynthesis[20] of melatonin, coenzyme Q10 and some neurotransmitters for liver functions, cellular replication and detoxifications. In most organisms, betaine is biosynthesized by the two-step oxidation of choline with two enzymes, choline dehydrogenase and betaine aldehyde dehydrogenase.[20] Demethylation of betaine yields DMG which can be further converted to sarcosine with dimethylglycine dehydrogenase.[21] In fact, DMG is also a byproduct of homocysteine metabolism whereas sarcosine can also be biosynthesized from glycine with glycine-*N*-methyl transferase.[21] More recently, sarcosine has been found to be a biomarker for invasive prostate cancer with its concentration in urine positively correlated with prostate cancer progression and metastasis[22] although this finding is currently under debate.[23]

The structural features and molecular dynamics of these metabolites ought to be important research topics given their biological importance. The crystal structure of sarcosine at 135 K showed an orthorhombic lattice with the space group of $P2_12_12_1$ and four different molecules in its unit cell.[24] The results from matrix-isolation FT-IR spectroscopy and molecular orbital calculations[25] have shown four conformers for sarcosine in the gaseous phase with experimentally accessible populations. At the ground conformational state, the N−C bond and the N−C−C═O axis adopt anti and syn arrangement, respectively, whereas the carboxylic moiety has cis conformation.[25] A proton-relaxation study of tris-sarcosine calcium-chloride revealed[26] the reorientation of CH_3 groups as the dominant motion. For DMG, the results from the matrix-isolation FT-IR and molecular orbital calculations[27] have shown three conformers in the neutral form. The conformational ground state has the intramolecularly O−H···N hydrogen-bond form where the (lone pair)−N−C−C and N−C−C═O dihedral angles are about 30° (gauche) and 180° (anti), respectively, while the carboxylic group adopts the trans configuration[27] with O═C−O−H dihedral angle of about 180°. So far, neither molecular dynamics nor crystal structural information is available for DMG.

Betaine anhydrous crystals showed the orthorhombic space group *Pnma* with four molecules in its unit cell,[28] whereas betaine hydrochloride crystals had monoclinic space group of $P2_1/c$ with two different forms, one of which had four molecules in one cell[29] and the other had two molecules in one cell.[30] Solid state NMR studies indicated that the molecular motions of betaine phosphate,[31] betaine phosphite[32] and their mixed systems[33] were dominated by the 3-fold methyl group rotations and whole trimethylamine group in the betaine moiety. However, so far there has been no report on the molecular dynamics of sarcosine, DMG, betaine and betaine hydrochloride themselves.

In order to understand the molecular dynamics and its structure dependences for the N-methylated glycines, in this report, we conducted a comprehensive study on the molecular motions of sarcosine, DMG, betaine anhydrous, and betaine hydrochloride using a catalogue of solid state NMR techniques including ^1H and ^{13}C relaxation time measurements, high resolution ^{13}C CPMAS NMR and dipolar and chemical shift correlation experiments (DIPSHIFT).

2. EXPERIMENTAL SECTION

2.1. Materials. Sarcosine, DMG, betaine anhydrous and betaine hydrochloride were all purchased from Sigma-Aldrich with quoted purities as 99% or 98%, and used without further purification. Their melting points were 208, 189, 245, and 300 °C, respectively, according to Sigma data. Figure 1 shows the molecular structures of them. Prior to experiments, these samples were dried over P_2O_5 in a desiccator under vacuum for at least 1 week. They were then packed into 4 mm NMR rotors and 10 mm NMR tubes respectively for 300 MHz high resolution and 20 MHz low resolution solid state NMR experiments.

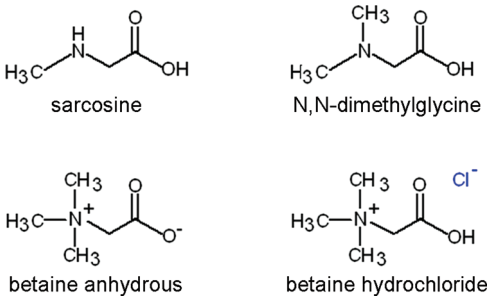

Figure 1. Molecular structures of sarcosine, DMG, betaine anhydrous, and betaine hydrochloride.

2.2. Differential Scanning Calorimetry (DSC) Studies. DSC analyses of sarcosine, DMG, betaine, and betaine hydrochloride were performed on a Pekin-Elmer Pyris 1 calorimeter in a sealed aluminum pan for each sample (about 5 mg). The temperature range was between 123 K and sample's melting point except for betaine hydrochloride, which was measured between 153 K and its melting point. The measurements were carried out using boiled liquid nitrogen as the cooling gas and helium as the purge gas with heating process recorded first followed with the cooling process. The heating and cooling rates were set to 10 K/min.

2.3. High Resolution Solid-State NMR Spectroscopy. The high resolution solid-state NMR experiments were carried out on a Varian Infinity Plus 300 spectrometer operating at 299.75 and 75.38 MHz for ^1H and ^{13}C, respectively. Samples were normally spun at 4−5 kHz in a 4 mm ZrO_2 rotor unless stated otherwise and the 90° pulse length was 2.4 μs for ^1H. For ^{13}C CP/MAS NMR experiments, the Hartmann−Hahn matching condition was set at the ambient temperature for each sample and the contact time varied between 1 and 2.5 ms to obtain the best S/N ratio. The acquisition time was limited to 60 ms with proton decoupling field strength of about 60 kHz to avoid stresses to hardware. The ^{13}C chemical shifts were referenced to the methyl group of a solid hexamethylbenzene sample externally (17.35 ppm for methyl group).

The ^{13}C T_1 was measured using the Torchia sequence[34] as a function of temperature with 14 relaxation delays (5 ms to 3 s) used for CH_3 groups and 12 relaxation delays (0.1−60 s) for CH_2 and CO groups. The data were then fitted to an exponential decay function to extract ^{13}C T_1 values.

The strength of the $^{13}C-^1H$ dipolar couplings was measured using the constant time 1D-DIPSHIFT[3] pulse sequence at various temperatures. The phase modulated Lee−Goldburg (PMLG)[35] pulse sequence was used for $^1H-^1H$ homonuclear decoupling. The spin speed was 4 kHz for DMG and betaine while 5 kHz for sarcosine and betaine hydrochloride to ensure complete cycles in one rotor period for the PMLG sequence. The signal over one rotor period in the indirect dimension was acquired, and therefore, DIPSHIFT spectra were only Fourier transformed in the direct dimension. The dipolar dephased signals were extracted for each resolved peak. The time evolution under the C−H dipolar couplings was simulated for one rotor

period using a home-built Fortran program kindly provided by Dr. Detlef Reichert. Simulations were performed for varying C−H dipolar coupling strengths, and other input parameters included the number of t_1 increments and spinning rate. The calculated curves were multiplied with an exponential decay function to account for T_2 relaxation effects during the time evolution. In DIPSHIFT spectra, the measured dipolar-coupling values were reduced by the scaling factor for the homonuclear decoupling sequence. Since scaling factors have been reported to vary significantly with the experimental conditions,[36] the $^{13}C-^{1}H$ dipolar coupling of CH and CH_3 moieties in alanine and CH_2 moiety in glycine obtained from DIPSHIFT spectra measured under the same condition were used as references.

For measurements of the principal values of chemical shift anisotropy (CSA), the spinning sidebands (SSB) were obtained from ^{13}C CP/MAS NMR spectra at spin rates varying from 0.8 kHz to 1.5 kHz. The principal values (δ_{11}, δ_{22}, and δ_{33}) were obtained using the Herzfeld-Berger method.[37]

2.4. Proton Relaxation Time Measurements. Proton spin−lattice relaxation time in the laboratory frame, T_1, was measured using the inversion−recovery pulse sequence (recycle delay−180°−τ−90°−acquisition) except the long T_1 (T_1 > 2 s) which was measured using the saturation−recovery pulse sequence (recycle delay−90°−τ−90°−acquisition) on a Bruker Mq-20 spectrometer (19.95 MHz). T_1 was also measured indirectly using the CP/MAS based pulse sequence on a Varian Infinity Plus 300 spectrometer (299.75 MHz). To ensure a sufficient spread of τ values for possible existence of multiexponential relaxation, the relaxation delay τ was adjusted[14] according to $\tau = A \times 10^{(m-1)/12}$, where A was a constant of 1−4 ms depending on the length of T_1 and m is the number of data points. The τ values were ranged from 40 μs to 40 s with 16−20 data points. The relaxation processes for all these compounds were found to be monoexponential within experimental error in the whole temperature range studied.

Proton spin−lattice relaxation time in the rotating frame, $T_{1\rho}$, was measured on a Bruker Mq-20 spectrometer. The standard sequence (recycle delay-90°-spin lock-acquisition)[38] was used with spin-lock time not longer than 300 ms when the spin-lock field strength was 45 kHz. 16−20 spin-lock times were used to obtain the $T_{1\rho}$ values. The decays of nuclear magnetization for all these compounds were also found to be monoexponential within experimental error in the whole temperature range studied.

Proton second moment, M_{2r}, was measured using the solid echo pulse sequence $[90°_x-\tau_1-90°_y-\tau\text{-AQ}]$[39] on a Bruker Mq-20 spectrometer to obtain the complete Bloch decay signal.[40] τ_1 was 13 μs and τ was chosen to be (11 μs) just slightly longer than the dead time of the spectrometer to ensure observation of an echo. The decay part of the solid echo was fitted to a modified Gaussian function to obtain the values of M_{2r}.[13,41]

All variable-temperature experiments were started from the lowest temperature with an increment of 10 K. A total of 15 min waiting time for each temperature was allowed to ensure temperature stabilization and equilibration with temperatures stabilized within ±1 K. The actual sample temperatures on Varian Infinity Plus 300 spectrometer were calibrated with ^{207}Pb chemical shift of $Pb(NO_3)_2$ as reported before[42] whereas the temperatures on Bruker Mq-20 spectrometer were calibrated by directly inserting a precalibrated thermal couple into a sample-filled tube in the probe head.

All relaxation time values were extracted by curve-fitting using a Ladenburg-Marquardt nonlinear curve-fitting routine on a personal computer.

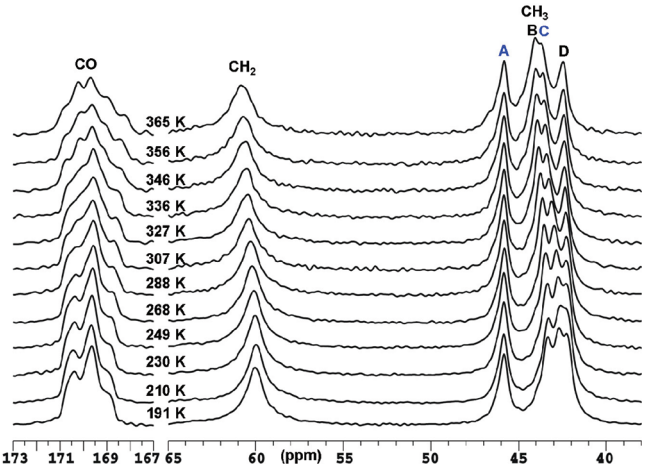

Figure 2. ^{13}C CP/MAS NMR spectra for DMG at various temperatures.

3. RESULTS AND DISCUSSION

3.1. Differential Scanning Calorimetry (DSC). The DSC curves of sarcosine, betaine anhydrous, and betaine hydrochloride showed no endothermic or exothermic process except melting whereas the DSC heating curve of DMG (Figure S1) showed a solid−solid phase transition at about 348.5 K with an enthalpy of 7.0 kJ/mol, which was not reported before. The peak of its melting process was at 449.9 K with an enthalpy of 19.6 kJ/mol.

3.2. ^{13}C CP/MAS NMR Spectra. The ^{13}C CPMAS spectra of N-methylated glycines at different temperatures showed some interesting features. At room temperature, sarcosine (Figure S2) showed three signals at 172.7, 50.9, and 31.8 ppm for CO, CH_2, and CH_3 moieties, respectively. In the temperature range of 181−336 K, their line-shapes had little changes although there was a small but obvious change of chemical shifts, which will be discussed later. At 190−365 K, DMG showed four signals for CH_3 (namely, A, B, C and D) (Figure 2) whereas such multiplicity was not obvious for CH_2 (60.5 ppm). This together with the presence of multiple signals for the carbonyl group indicated that there might be four nonequivalent molecules in the unit cell probably due to packing. Furthermore, at the ambient temperature, methyl groups A and C had proton T_1 values of about 450 and 397 ms (at 300 MHz) respectively and $T_{1\rho}$ values longer than 300 ms (with spin-lock field of 67 kHz); B and D had T_1 values of about 620 ms and $T_{1\rho}$ values of 18 ms (Figure S3). This indicated that spin diffusion was not efficient enough for these two groups of methyl groups even at the time scale of T_1 (up to 620 ms) and further supported the presence of multiple nonequivalent molecules in the unit cell. Although line-shapes for the CO signals had some slight changes with the temperature increase, the line-shapes for CH_2 and CH_3 signals had no obvious changes. Moreover, no drastic changes were observable accompanied with the phase transition around 350 K although B and C showed clear downfield shifts (chemical shifts underwent some clear increases). Unfortunately, so far, there is no crystal structure available for DMG.

The ^{13}C CP/MAS NMR spectra of betaine anhydrous (Figure 3a) showed two resonance lines below 278 K at 56.0 ppm (A) and 50.6 ppm (B) for methyl groups with the peak-area ratio of 1:2. However, these two peaks coalesced into a single resonance at about 52.9 ppm (C) when temperature was above 297 K. This implies that one of three CH_3 groups (A) in the trimethylamine

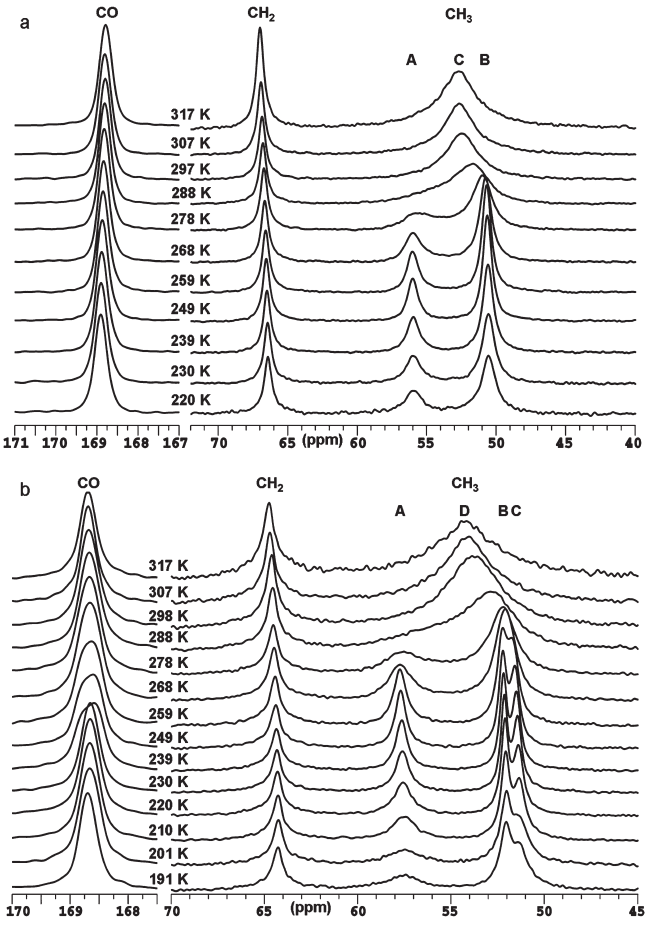

Figure 3. ^{13}C CP/MAS NMR spectra for betaine anhydrous (a) and betaine hydrochloride (b) at various temperatures.

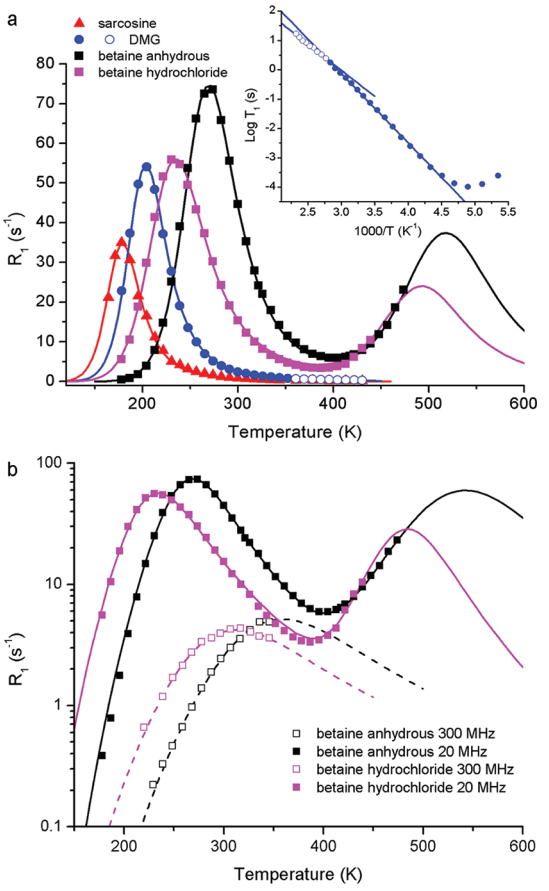

Figure 4. Temperature dependence of proton spin−lattice relaxation rate in the laboratory frame for sarcosine, DMG, betaine anhydrous and betaine hydrochloride at 20 MHz (a), and for betaine anhydrous and betaine hydrochloride at 20 and 300 MHz (b). The inset shows the log T_1 versus $1000/T$ for DMG. Solid and dashed lines are fitted data.

group has different chemical environment from the other two CH_3 groups (B), which is consistent with the X-ray diffraction results.[28] When sample temperature reaches a certain level, the trimethylamine group rotates fast enough to make all three methyl groups have an averaged chemical environment leading to coalescence of their ^{13}C NMR signals. The line-shapes of CO and CH_2 groups did not change much over the temperature range studied.

The ^{13}C CP/MAS NMR spectra of betaine hydrochloride (Figure 3b) showed that below 259 K there were three resonance lines A (57.5 ppm), B (52.1 ppm), and C (51.4 ppm) for methyl groups with the peak-area ratio of about 1:1:1. When temperature reached about 268 K, B and C coalesced to form a single peak with A obviously broadened. The coalescence of three methyl peaks continued with broadening of their signals. When temperature reached 298 K, all three signals from methyl groups coalesced completely as a single peak D (54.3 ppm). This indicated that at low temperature the chemical environments were different for all three methyl groups being in good agreement with the X-ray crystallographic data.[29] With the rise of sample temperature, the thermally enhanced rotation of whole trimethylamine group was promoted leading to the average of their chemical environments. The signal broadening for A−C during this process probably resulted from the rotational exchanges of three methyl groups. The line-shapes of CH_2 group did not change much over the temperature range studied as in the case of betaine anhydrous.

Some further changes of chemical shifts as a function of temperature were also observed for these four molecules apart from above-discussed. For all them, CH_2 signal showed downfield shifts with the increase of temperature whereas carbonyl (CO) signals showed little changes. The temperature dependence for chemical shifts of CH_3 groups was more diverse. With the rise of temperature, methyl group of sarcosine showed a downfield shift. Similar observation was made for signals of B and C in the case of DMG whereas A and D peaks showed little changes. Similar variations of chemical shift with temperature have been reported for α-glycine,[43] *n*-alkanes, and polyethylene,[44] probably due to temperature effects on the chemical bond distances or spacing between crystal-faces[43,44] and thus on the inter- and intramolecular interactions.

3.3. Proton Spin−Lattice Relaxation in the Laboratory Frame. Figure 4 shows the proton spin−lattice relaxation rates in the laboratory frame, R_1, as a function of temperatures for sarcosine, DMG, betaine and betaine hydrochloride. R_1 maxima attributable to the 3-fold rotation of CH_3 group were observed for all these N-methylated glycines although the positions of these maxima were different for different molecules. At 20 MHz, for instance, sarcosine, DMG, betaine and betaine hydrochloride showed such maximum at about 180 K, 203 K, 274 and 230 K respectively. This implies that the methyl groups in these molecules have obvious differences in terms of their molecular dynamics. At

dx.doi.org/10.1021/jp2104374 |*J. Phys. Chem. B* 2012, 116, 136–146

300 MHz, the methyl rotation related R_1 maximum moved to higher temperature at about 359 K for betaine anhydrous and 314 K for betaine hydrochloride, respectively.

DMG only showed a single maximum for the CH_3 reorientation even though there were two methyl groups in DMG and two nonequivalent molecules in its unit cell. This implies that the motional properties of two methyl groups in a single DMG molecule and two different molecules in its unit cell are not drastically different. However, log T_1 as a function of reciprocal of temperature showed that there was a discontinuity in T_1 at about 355 K (inset in Figure 4a). This is probably related to the solid−solid phase transition at 348.5 K observed from DSC. For R_1 of both betaine anhydrous and betaine hydrochloride at 20 MHz, another relaxation peak appeared at the temperature above 420 K though not reached their maxima. This indicates the presence of yet another efficient proton relaxation process probably attributable to the rotation of the whole trimethylamine group around the N−C bond.

To evaluate these motions quantitatively, the experimental data for sarcosine and DMG were fitted to the well-known Kubo−Tomita expression (eq 1)[45,46] assuming exponential correlation function

$$R_1 = \frac{1}{T_1} = \sum_{i \geq 1} C_i \left[\frac{\tau_{ci}}{1 + \omega_0^2 \tau_{ci}^2} + \frac{4\tau_{ci}}{1 + 4\omega_0^2 \tau_{ci}^2} \right] \quad (1)$$

where ω_0 is the proton Larmor frequency and τ_{ci} is the rotational correlation time of the motions responsible for the spin−lattice relaxation, which is assumed to follow the Arrhenius activation law

$$\tau_{ci} = \tau_{0i} \exp\left(\frac{E_{ai}}{RT}\right) \quad (2)$$

where τ_{0i} is the pre-exponential factor corresponding to the rotational correlation time at infinite temperature, E_{ai} is the activation energy and R is the gas constant. C_i is the relaxation constant given by eq 3 assuming that the motion occurring is fast on the NMR relaxation time scale

$$C_i = \frac{9}{20} \frac{n_i}{N_i} \frac{\gamma^4 \hbar^2}{r^6} \quad (3)$$

where γ is the proton magnetogyric ratio. N_i is the total number of protons in the molecule, n_i is the number of protons contributing to the relaxation process, and r is the average interproton distance in motional groups.

For betaine and betaine hydrochloride at 300 MHz, only the methyl group rotation process was observed in the temperature range studied and the data was also analyzed by the above Kubo−Tomita equation. For their R_1 at 20 MHz, both the rotations of three individual methyl groups and the whole trimethylamine group were observed. In such cases, Dunn−McDowell equation (eqs 4 and 6)[47] were employed to take consideration of the intra- and intermethyl relaxations assuming configuration of nitrogen in both betaine anhydrous and betaine hydrochloride as tetrahedral.[48]

$$\frac{1}{T_1(\text{intramethyl})} = \frac{9}{80} N \frac{\gamma^4 \hbar^2}{r^6} \left[\frac{32}{27} f(\omega_0 \tau_1) + \frac{32}{27} f(\omega_0 \tau_2) + \frac{76}{27} f(\omega_0 \tau_3) \right] \quad (4)$$

where N is the ratio of number of proton in methyl groups and that in whole molecule, i.e., 9/11 and 3/4 for betaine anhydrous and betaine hydrochloride, respectively. r is the average interproton distance in the methyl group. τ_1 and τ_2 are the correlation times for C_3 reorientation of methyl group and 3-fold reorientation of whole trimethylamine group, respectively, and $\tau_3^{-1} = \tau_1^{-1} + \tau_2^{-1}$. Correlation times are assumed to follow the Arrhenius activation law as well as shown in eq 2. $f(\omega_0 \tau_i)$ is the spectral density function given by eq 5.

$$f(\omega_0 \tau_i) = \frac{\tau_i}{1 + \omega_0^2 \tau_i^2} + \frac{4\tau_i}{1 + 4\omega_0^2 \tau_i^2} \quad (5)$$

The intermethyl relaxation rate is approximated by the relation stated in eq 6.

$$\frac{1}{T_1(\text{intermethyl})} = \frac{27}{20} N \frac{\gamma^4 \hbar^2}{r^{*6}} f(\omega_0 \tau_2) \quad (6)$$

where r^* is the average distance between the centers of the methyl groups.

For all four N-methylated glycines, the experimental data agreed satisfactorily with the theoretical ones (Figure 4). The relaxation parameters for the different motions obtained from the curve-fittings are tabulated in Tables 1 and 2.

For sarcosine, the methyl group rotation is characterized with E_a of 18.0 kJ/mol and a τ_0 value of 2.8×10^{-14} s. This is in accord with those for the commonly encountered methyl groups such as in amino acids[6−8] and α-L-fucopyranose[13] although the E_a value is larger and the τ_0 value is smaller than those of CH_3 rotation in tris-sarcosine calcium-chloride[26] ($E_a \approx 12.5$ kJ/mol, $\tau_0 \approx 1.9 \times 10^{-13}$ s). The relaxation constant (C) of methyl group for sarcosine is about 3.06×10^9 rad s^{-2}. Assuming the protons in the methyl group as equilateral and the major contributor to relaxation, the calculated average interproton distance in the methyl group is about 1.816 (±0.004) Å according to eq 3. This is also in reasonable agreement with such value for methyl group (1.80 Å) of tris-sarcosine calcium chloride.[26]

For DMG, obvious differences were observable for the methyl group rotation in the low and high temperature phases with E_a values of 19.9 and 14.7 kJ/mol, respectively, and the corresponding τ_0 values of 3.7×10^{-14} s and 2.3×10^{-13} s, respectively. In contrast, the relaxation constant for both phases were similar (4.76×10^9 and 4.28×10^9 rad s^{-2} for the low and high temperature phase, respectively) indicating that the phase transition was a solid-to-solid one. Both values were much larger than that for sarcosine (3.06×10^9 rad s^{-2}) confirming that the relaxation process in *N,N*-dimethylglycine was due to the rotation of both methyl groups. Although no crystal structure has been reported for *N,N*-dimethylglycine so far, the interproton distances for methyl group can be extracted tentatively from C values of methyl group. Assuming equilateral positioning for three protons in the methyl groups, the calculated average interproton distance in the methyl group is about 1.816 (±0.001) Å in the low temperature phase, which agrees with that in the methyl group of sarcosine. Assuming protons in the methyl groups adopt perfect equilateral geometry the calculated C−H bond length is 1.112 (±0.001) Å. For the time being, these are the only data available for the interproton distances in DMG although these results need confirming with results from neutron scattering.

For betaine anhydrous, E_a value for the rotation of methyl groups (25.0 kJ/mol) is considerably larger than those for the typical methyl groups.[6−8] However, such value is similar to those of methyl groups in multimethylated organic compounds such as

dx.doi.org/10.1021/jp2104374 | J. Phys. Chem. B 2012, 116, 136–146

Table 1. Relaxation Parameters for Sarcosine, DMG, Betaine Anhydrous, and Betaine Hydrochloride from Proton Spin−Lattice Relaxation Time in the Laboratory and Rotating Frames at 20 MHz

	activation energy E_a (kJ/mol)	τ_0 (10^{-14} s)	relaxation constant C (10^9 rad s^{-2})	$T_1^{min}/T_{1\rho}^{min}$ (ms)	temperature at T_1^{min} (K)
			Sarcosine		
T_1					
CH_3	18.0 ± 0.4	2.8 ± 0.6	3.06 ± 0.04	28.8	180
			N,N-Dimethylglycine		
T_1					
CH_3 (low temp phase)	19.9 ± 0.09	3.7 ± 0.2	4.76 ± 0.02	18.5	203
CH_3 (high temp phase)	14.7 ± 1.9	23 ± 3 × 10^4 [a]	4 ± 5 × 10^3 [a]	20.6	178
$T_{1\rho}$					
CH_3	21.2 ± 0.4	3.8 ± 0.9	4.76[b]	0.25	148
			Betaine Anhydrous		
T_1					
CH_3	25.0 ± 0.1	6.6 ± 0.3	6.56 ± 0.02	13.5	271
$N^+(CH_3)_3$	55.3 ± 3.5	2.3 ± 4.3	1.09 ± 1.61	16.8	544
$T_{1\rho}$					
CH_3	28.8 ± 0.7	0.5 ± 0.2	16.9 ± 0.2	0.07	181
$N^+(CH_3)_3$	53.5 ± 1.0	1.5 ± 0.5	0.43 ± 0.03	0.14	350
			Betaine Hydrochloride		
T_1					
CH_3	18.3 ± 0.2	40.1 ± 3.4	5.0 ± 0.04	17.9	232
$N^+(CH_3)_3$	74.4 ± 22.8	0.005 ± 0.05	0.32 ± 4.4	35.0	484
$T_{1\rho}$					
CH_3	19.9 ± 0.8	40.0 ± 20.9	5.0[b]	0.23	160
$N^+(CH_3)_3$	52.5 ± 0.4	1.6 ± 0.2	1.30 ± 0.01	0.17	346

[a] Large errors resulted from limited data points. [b] Values from T_1 data analysis used as constrains in data-fitting.

tetramethylammonium halides.[49] The E_a value for whole trimethylamine group rotation (55.3 kJ/mol) agreed well with those for similar groups in choline halides[50] although such value is much larger than those in betaine phosphate,[31] betaine phosphite[32] and their mixtures,[33,51] and acetylcholine chloride.[52] Such discrepancy may result from the differences in crystal packings and thus steric hindrance for the rotation of the whole trimethylamine group. The calculated average interproton distance for the methyl groups was 1.781 (±0.001) Å from the C value for methyl group rotation (6.56 × 10^9 rad s^{-2}). Although such distance differs considerably from that reported (1.665 Å) from X-ray data,[28] our data is in good agreement with such values in common methyl groups.[6−8] In fact, it is well-known that proton distances obtained from X-ray data is not reliable.

Assuming that the trimethylamine group adopted tetrahedral geometry (for nitrogen) and protons in each methyl group were equilateral, the calculated average distance between the centers of the methyl groups was about 2.402 Å based on the C value for the whole trimethylamine group rotation (1.09 × 10^9 rad s^{-2}). Such value is in good agreement with that from X-ray results which showed average C−C distance in trimethylamine group as 2.437 Å.

For betaine hydrochloride, the E_a value for methyl group rotation (18.3 kJ/mol) agreed well with those for the commonly encountered methyl groups[6−8] though smaller than that for betaine anhydrous. The E_a value for the whole trimethylamine group rotation (74.4 kJ/mol) is much greater than that for betaine anhydrous. Close inspection of the results (Table 1) revealed that error for this activation energy was much greater than that for betaine probably due to limited data points at the high temperature end. If this is true, then E_a value for this motion can be obtained more accurately from the $T_{1\rho}$ measurements since the relaxation peak will be moved to lower temperature in $R_{1\rho}$ data. The calculated average interproton distance in methyl groups was about 1.837 (±0.002) Å from the methyl group relaxation constant (5.0 × 10^9 rad s^{-2}), which is reasonable for methyl groups[6−8] but slightly larger than that in betaine anhydrous. The E_a and C values for methyl group rotations obtained from 300 MHz were broadly consistent with the results obtained from 20 MHz data for both betaine anhydrous (21.8 kJ/mol, 6.8 × 10^9 rad s^{-2}) and betaine hydrochloride (17.2 kJ/mol, 5.56 × 10^9 rad s^{-2}). The width of relaxation peak for methyl groups in this compound appears to be broader than those in the other three metabolites (Figure 4a). This will be further investigated with high resolution ^{13}C NMR techniques in the later section.

It is particularly interesting to note that the activation energy E_a and the time factor τ_0 for the methyl group rotations increase with the increase of the methyl group number in these four molecules (Figure 5). This is probably due to the steric hindrance induced-increases in the energy barrier for the methyl rotations. However, betaine hydrochloride did not follow such trend well probably due to different intramolecular interactions present in this molecule.

3.4. Proton Spin−Lattice Relaxation in the Rotating Frame. The proton spin−lattice relaxation rates in the rotating frame, $R_{1\rho}$, were also measured as a function of temperature (Figure S4) for

dx.doi.org/10.1021/jp2104374 |J. Phys. Chem. B 2012, 116, 136–146

Table 2. Relaxation Parameters for Sarcosine, DMG, Betaine Anhydrous, and Betaine Hydrochloride Obtained from ^{1}H T_1 at 300 MHz and ^{13}C T_1 at 75.38 MHz

	activation energy E_a (kJ/mol)	τ_0 (10^{-14} s)	relaxation constant κ/C (10^9 rad s^{-2})	T_1^{min} (ms)	temperature at T_1^{min} (K)
			Sarcosine		
^{13}C T_1					
CH_3	14.0 ± 0.5	26.6 ± 6.9	3.85 ± 0.07	66	193
			N,*N*-Dimethylglycine		
^{13}C T_1					
A CH_3	15.1 ± 0.5	20.4 ± 5.3	3.54 ± 0.08	72	202
B CH_3	13.9 ± 0.5	52.7 ± 12.0	4.29 ± 0.08	59	208
C CH_3	13.8 ± 0.4	44.3 ± 8.4	4.45 ± 0.08	57	202
D CH_3	13.9 ± 0.3	38.2 ± 5.2	4.19 ± 0.05	61	198
			Betaine Anhydrous		
^{1}H T_1					
CH_3	21.8 ± 0.7	21.5 ± 6.7	6.8 ± 0.2	194	359
^{13}C T_1					
A CH_3	20.6 ± 2.3	53.5 ± 53.2	4.3 ± 0.2	59	308
B CH_3	20.2 ± 1.1	63.0 ± 31.7	4.3 ± 0.1	59	308
			Betaine Hydrochloride		
^{1}H T_1					
CH_3	17.2 ± 0.5	42.8 ± 8.2	5.56 ± 0.06	238	314
^{13}C T_1					
A CH_3	20.5 ± 0.5	18.5 ± 4.4	3.74 ± 0.05	68	271
B CH_3	13.9 ± 0.5	211.3 ± 56.8	3.91 ± 0.07	65	250
C CH_3	15.8 ± 0.5	110.5 ± 27.0	3.82 ± 0.06	66	259

DMG, betaine anhydrous and betaine hydrochloride. The rise in $R_{1\rho}$ of DMG at lower temperatures indicated a maximum at about 144 K attributable to the reorientation of methyl groups. Betaine anhydrous showed two relaxation processes at about 180 and 350 K, whereas betaine hydrochloride showed one clear maximum at about 346 K and the rise in $R_{1\rho}$ at lower temperatures indicated another maximum at about 150 K. The low and high temperature maxima in betaine and betaine hydrochloride were attributed to the rotations of the methyl groups and the whole trimethylamine groups, respectively. We did not get the variable temperature $R_{1\rho}$ data for sarcosine since its $T_{1\rho}$ was too long to be measured over the temperature range studied.

For DMG, the $R_{1\rho}$ data were fitted to an expression as described in eq 7 assuming that the dipole−dipole interactions were the dominant relaxation mechanism[13,53]

$$R_{1\rho} = \frac{1}{T_{1\rho}} = \frac{3}{2}\sum_{i \geq 1} C_i \left[\frac{\tau_{ci}}{1 + 4\omega_{ei}^2\tau_{ci}^2} + \frac{5}{3}\frac{\tau_{ci}}{1 + \omega_0^2\tau_{ci}^2} + \frac{2}{3}\frac{\tau_{ci}}{1 + 4\omega_0^2\tau_{ci}^2}\right] \quad (7)$$

For betaine anhydrous and betaine hydrochloride, the $R_{1\rho}$ data were fitted to eqs 8 and 9 to take both intra- and intermethyl contributions into consideration[48]

$$\frac{1}{T_{1\rho}(\text{intramethyl})} = \frac{9}{80}N\frac{\gamma^4\hbar^2}{r^6}\left[\frac{32}{27}f_\rho(\omega_e, \omega_0\tau_1) + \frac{32}{27}f_\rho(\omega_e, \omega_0\tau_2) + \frac{76}{27}f_\rho(\omega_e, \omega_0\tau_3)\right] \quad (8)$$

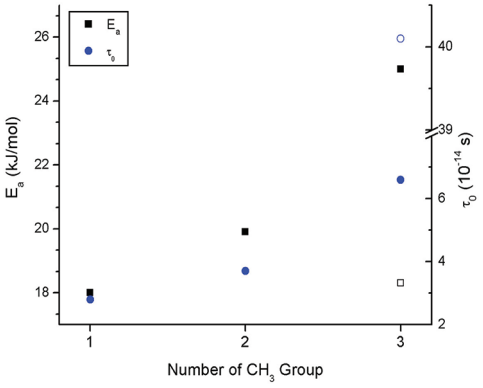

Figure 5. E_a and τ_0 values for methyl group rotation as a function of the number of substituted methyl groups in sarcosine, DMG, betaine anhydrous, and betaine hydrochloride.

$$\frac{1}{T_{1\rho}(\text{intermethyl})} = \frac{27}{20}N\frac{\gamma^4\hbar^2}{r^{*6}}f_\rho(\omega_e, \omega_0\tau_2) \quad (9)$$

$f_\rho(\omega_e,\omega_0\tau_i)$ is the spectral density function given as

$$f_\rho(\omega_e, \omega_0\tau_i) = \frac{3}{2}\frac{\tau_i}{1 + 4\omega_e^2\tau_i^2} + \frac{5}{2}\frac{\tau_i}{1 + \omega_0^2\tau_i^2} + \frac{\tau_i}{1 + 4\omega_0^2\tau_i^2} \quad (10)$$

where ω_0, τ_{ci}, C_i, and τ_i have the same meaning as in the previous expressions and ω_e is the effective field for relaxation in frequency

dx.doi.org/10.1021/jp2104374 |*J. Phys. Chem. B* 2012, 116, 136–146

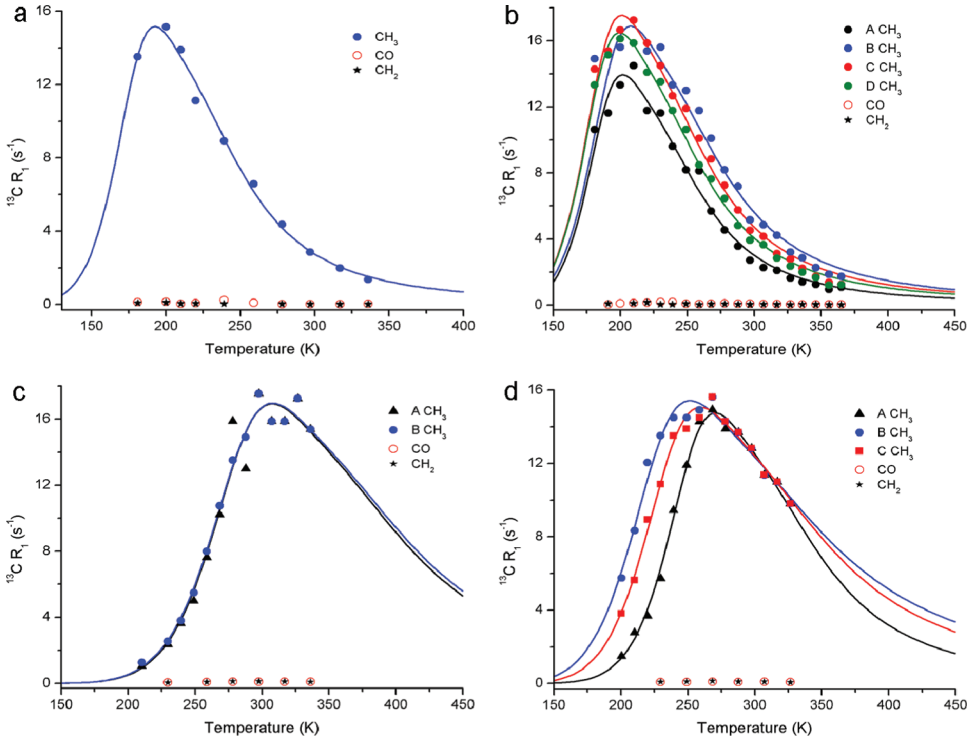

Figure 6. Temperature dependence of ^{13}C spin−lattice relaxation time in the laboratory frame for sarcosine (a), DMG (b), betaine anhydrous (c), and betaine hydrochloride (d). Lines are fitted data.

unit. Since the spin-lock field (ω_{SP}, about 45 kHz) and the local dipolar field strength (ω_L, about 50 kHz) were similar in this study, these two terms were taken into consideration using the McCall−Douglass equation[54] (eq 11)

$$\omega_e = \sqrt{{\omega_{SP}}^2 + {\omega_L}^2} \tag{11}$$

For DMG, ω_L was 54 kHz over the temperature range studied, whereas for betaine anhydrous and betaine hydrochloride, ω_L showed some temperature dependence. Nevertheless, ω_L was modeled satisfactorily by a double-sigmoid and a single-sigmoid function respectively for betaine and its hydrochloride salt within the temperature range used.

The relaxation parameters were obtained by fitting the experimental data to the above equations (Figure S4) and shown in Table 1. Due to limited data points at the low temperature end, the methyl group relaxation constants for DMG and betaine hydrochloride were constrained to those obtained from R_1 results. The obtained E_a values for most of the relaxation processes agreed well with those obtained from R_1 analysis. Although the E_a value (52.5 kJ/mol) for the whole trimethylamine group rotation in betaine hydrochloride here was smaller than the results from the R_1 analysis (74.4 kJ/mol), the R_1 analysis results clearly had much greater error (see Table 1) probably resulting from limited data points in the case of R_1 analysis.

3.5. ^{13}C Spin−Lattice Relaxation in the Laboratory Frame (^{13}C T_1). We further measured the ^{13}C T_1 as a function of temperature (181−365 K) for each carbon in sarcosine, DMG, betaine anhydrous and betaine hydrochloride (Figure 6). The results showed that, for all these four metabolites, ^{13}C T_1 of methyl groups was much shorter than that of methylene and carbonyl groups probably due to their 3-fold reorientations. These data are further analyzed quantitatively using eq 12 assuming the proton-carbon dipolar interactions as the dominant relaxation source[13]

$$\frac{1}{T_1} = \kappa\left[\frac{\tau_c}{1 + (\omega_P - \omega_C)^2\tau_c^2} + \frac{3\tau_c}{1 + \omega_C^2\tau_c^2} + \frac{6\tau_c}{1 + (\omega_P + \omega_C)^2\tau_c^2}\right] \tag{12}$$

where ω_P and ω_C are the Larmor frequencies for ^1H and ^{13}C, respectively. τ_c is the same as in eq 2, and κ is the relaxation constant, which can be expressed as in eq 13

$$\kappa = \frac{3}{10}\left(\frac{\mu_0}{4\pi}\right)^2 {\gamma_P}^2{\gamma_C}^2\hbar^2{r_{PC}}^{-6} \tag{13}$$

where r_{PC} is the mean C−H bond length, γ_P and γ_C are the magnetogyric ratios for ^1H and ^{13}C, respectively. Assuming that protons in the methyl groups adopt perfect equilateral geometry and based on the mean interproton distances obtained from R_1 results, the values for κ are estimated to be 5.72×10^9, 5.72×10^9, 6.4×10^9, and 5.33×10^9 rad s^{-2} respectively for methyl groups in sarcosine, DMG, betaine anhydrous, and betaine hydrochloride.

Figure 6 showed that the experimental data for all these methyl groups agreed well with the calculated ones in the temperature range studied and the fitted results were tabulated in Table 2. These results indicated that methyl groups in these four metabolites had their own unique dynamic properties. In sarcosine, E_a, τ_0 and κ values for methyl group rotation are 14 kJ/mol, 2.66×10^{-13} s, and 3.85×10^9 rad s^{-2}, respectively. In DMG, four

dx.doi.org/10.1021/jp2104374 |J. Phys. Chem. B 2012, 116, 136–146

Table 3. Principal Values of CSA Tensors for Sarcosine, *N,N*-Dimethylglycine, Betaine Anhydrous, and Betaine Hydrochloride[a]

	δ_{iso} (ppm)	δ_{33} (ppm)	δ_{22} (ppm)	δ_{11} (ppm)	$\lvert\delta_{33} - \delta_{11}\rvert$ (ppm)	$\Delta\delta$ (ppm)	η
				Sarcosine			
CO (298 K)	172.7	241.7 ± 0.9	166.6 ± 1.2	109.8 ± 0.4	131.9 ± 0.7	103.5 ± 1.3	0.82 ± 0.03
CH_2 (298 K)	50.9	17.1 ± 1.2	56.5 ± 1.4	79.1 ± 2.0	61.9 ± 3.1	−50.7 ± 1.9	0.67 ± 0.08
CH_3 (298 K)	31.8	5.1 ± 3.4	42.6 ± 5.1	47.7 ± 1.7	42.6 ± 1.7	−40.0 ± 5.1	0.21 ± 0.28
				N,N-Dimethylglycine			
CO (298 K)	170.3	245.3 ± 0.1	155.9 ± 0.0	109.7 ± 0.1	135.6 ± 0.1	112.5 ± 0.1	0.62 ± 0.00
	169.6	246.0 ± 0.0	150.8 ± 0.2	112.0 ± 0.2	134.0 ± 0.1	114.6 ± 0.1	0.51 ± 0.01
CH_2 (298 K)	60.5	27.0 ± 1.6	70.6 ± 2.9	83.9 ± 1.3	56.9 ± 0.2	−50.2 ± 2.3	0.40 ± 0.14
CH_3 (298 K)	46.1	13.4 ± 1.3	60.1 ± 4.0	64.8 ± 2.7	51.5 ± 1.4	−49.1 ± 1.9	0.15 ± 0.21
	44.0	10.1 ± 1.7	53.5 ± 2.0	68.3 ± 0.3	58.2 ± 1.4	−50.8 ± 2.5	0.44 ± 0.09
	43.5	9.2 ± 1.8	52.9 ± 1.7	68.4 ± 0.2	59.3 ± 2.0	−51.5 ± 2.8	0.46 ± 0.07
	42.6	10.4 ± 1.7	56.9 ± 3.4	60.6 ± 1.7	50.2 ± 0.0	−48.4 ± 2.6	0.12 ± 0.17
				Betaine Hydrochloride			
CO (298 K)	168.5	257.6 ± 0.8	142.6 ± 2.1	105.4 ± 1.3	152.2 ± 0.5	133.6 ± 1.2	0.42 ± 0.04
CH_2 (298 K)	64.4	32.8 ± 0.8	76.1 ± 3.7	84.3 ± 4.6	51.5 ± 5.4	−47.4 ± 1.3	0.25 ± 0.25
				Betaine Anhydrous			
CO (298 K)	168.9	244.7 ± 0.6	148.9 ± 0.0	113.0 ± 0.8	131.7 ± 1.4	113.7 ± 1.0	0.47 ± 0.01
CO (300 K)	168.9	245.5	151.2	110.1	135.4	114.85	0.537
CO (318 K)	168.9	245.9	149.9	110.8	135.1	115.55	0.508
CO (338 K)	168.9	245.8	150.8	110.1	135.7	115.35	0.53
CO (358 K)	168.9	244.0	150.5	112.2	131.8	112.65	0.51
CH_2 (298 K)	66.8	33.6 ± 1.6	78.3 ± 1.8	88.8 ± 0.1	55.3 ± 1.8	−50.0 ± 2.6	0.32 ± 0.07

[a] The SD values were obtained from results acquired at different spin rates.

methyl groups (A−D) all have similar E_a, τ_0 and κ values within the margin of error indicating that they have similar dynamic properties even though they are nonequivalent in their environment. Similarly, all methyl groups in betaine anhydrous have similar rotational properties with similar E_a, τ_0, and κ values. In contrast, for betaine hydrochloride, three methyl groups have fairly different E_a values (i.e., 20.5 kJ/mol for A, 13.9 kJ/mol for B, and 15.8 kJ/mol for C). While methyl A had similar activation energy to that of methyl groups in betaine anhydrous, E_a values for the other two methyl groups (B and C) were clearly smaller. Furthermore, the τ_0 value for methyl group A (1.85×10^{-13} s) was 1 order of magnitude smaller than those for the other two methyl groups (2.1×10^{-12} s for B and 1.1×10^{-12} s for C). This implies that the rotational motions of these three methyl groups in betaine hydrochloride are distinctively different from each other. This further suggests that their relaxation maxima have been overlapped in proton R_1 (Figure 4a) probably due to the limited resolution there. This was probably why the width of methyl group relaxation peak for betaine hydrochloride in R_1 was broader that those for the other three molecules (Figure 4a). The relaxation constants of A, B, and C methyl groups in betaine hydrochloride (3.74×10^9, 3.91×10^9, and 3.82×10^9 rad s^{-2}, respectively) were all smaller than the calculated ones. In fact, such notion is also valid for all the other N-methylated glycines studied here. Although the exact reasons are not certain, underestimation of H−C bond lengths is at least one possibility with the assumption of perfect equilateral geometry for methyl groups. The other possibility is the contributions from the intermethyl dipolar interactions and dipole−dipole interactions between protons in methyl groups and other protons.

3.6. ^{13}C Chemical Shift Anisotropy (CSA). ^{13}C chemical shift anisotropy is another useful NMR parameter for characterizing molecular dynamics. The chemical shift anisotropy is reduced in the presence of motions occurring at frequencies faster than the magnitude of the CSA interactions. For the sake of clarity, in the following discussion, we will use a deshielding convention for CSA. Therefore, the principal components are denoted as δ_{11}, δ_{22}, and δ_{33} and ordered with $|\delta_{33} - \delta_{iso}| \geq |\delta_{11} - \delta_{iso}| \geq |\delta_{22} - \delta_{iso}|$, where δ_{iso} is the isotropic chemical shift and defined as

$$\delta_{iso} = (\delta_{11} + \delta_{22} + \delta_{33})/3 \quad (14)$$

From these components, the shielding anisotropy $\Delta\delta$ can be defined as

$$\Delta\delta = \delta_{33} - (\delta_{11} + \delta_{22})/2 \quad (15)$$

and the asymmetry parameter η are defined as

$$\eta = (\delta_{22} - \delta_{11})/(\delta_{33} - \delta_{iso}) \quad (0 \leq \eta \leq 1) \quad (16)$$

The principal components of CSA tensors are tabulated in Table 3 for sarcosine, DMG, betaine anhydrous, and betaine hydrochloride. These values for CO moieties in sarcosine and betaine hydrochloride are consistent with the previously reported ones.[55] The CSA span $|\delta_{33} - \delta_{11}|$ of carbonyl groups in sarcosine, DMG and betaine anhydrous are all about 130 ppm (Figure S5) being similar to the values of those moieties in glycine,[55] leucine[56] and norvaline[57] (134, 134, and 134.5 ppm, respectively). However, $|\delta_{33} - \delta_{11}|$ value of carbonyl group in betaine hydrochloride is about 150 ppm obviously larger than the values in sarcosine, DMG, and betaine anhydrous due possibly to the effects of chloride ion.

In contrast, $|\delta_{33} - \delta_{11}|$ values for CH_2 and CH_3 in all these four molecules are similar (about 45−60 ppm). In fact, these

dx.doi.org/10.1021/jp2104374 |J. Phys. Chem. B 2012, 116, 136–146

values are also similar to that for those groups in glycine[58] and leucine[56] but larger than that for those moieties in D,L-norvaline[57] where CH_2 and CH_3 groups have additional motions apart from the 3-fold rotation of CH_3. Furthermore, $|\delta_{33} - \delta_{11}|$ values for carbonyl group of betaine anhydrous did not change much in the temperature range of 300−358 K, which is similar to what has been observed in norvaline due to limited slow motions for this group.

3.7. Dipolar Couplings and Chemical Shift Correlation (DIPSHIFT). The $^{13}C-^{1}H$ dipolar dephasing curves for CH_2 and CH_3 moieties in all four N-methylated glycines (Figure S6) showed behavior similar to these moieties in alanine and glycine, respectively, in the whole temperature range studied. This indicates that motional properties of CH_2 groups in the four molecules are similar to CH_2 in glycine. This also suggests that there are no additional fast motions for CH_3 apart from their 3-fold rotation and the whole trimethylamine group rotations in two betaines. The presence of chloride has no significant effect on the dipolar coupling of CH_3 groups probably because chloride anion is interacted with the carboxylic group via Cl···H−O−CO− hydrogen bonding as shown in its crystal structure.[29]

4. CONCLUSIONS

The 3-fold rotation of CH_3 groups is a common relaxation process in all four N-methylated glycines, namely sarcosine, *N*,*N*-dimethylglycine, betaine, and betaine hydrochloride, whereas whole trimethylamine rotation is a common motion in betaine and its chloride salt. Unique motional processes are also present for different molecules. Both methyl groups in DMG showed similar motional properties even though four different methyl groups (in different environments) were present there. A solid−solid phase transition was present for DMG at about 348.5 K and rotational properties of methyl groups were obviously different in these two different phases. Furthermore, three methyl groups in betaine showed similar motional properties whereas three methyl groups in betaine hydrochloride showed fairly different motional properties. The molecular dynamics of CH_2 moieties in the four molecules were similar to CH_2 moiety in glycine. Moreover, results from sarcosine, DMG and betaine anhydrous showed that the activation energy E_a and time factor τ_0 of CH_3 rotation increased with the rise of the number of substituted methyl groups.

■ ASSOCIATED CONTENT

Supporting Information. DSC data for DMG, ^{13}C CP/MAS NMR spectra for sarcosine, relaxation curves for methyl groups in DMG, temperature dependence of proton spin−lattice relaxation rate in the rotating frame for DMG, betaine anhydrous and betaine hydrochloride, the CSA span $|\delta_{33} - \delta_{11}|$ for different groups in sarcosine, DMG, betaine anhydrous and betaine hydrochloride, and DIPSHIFT information. This material is available free of charge via the Internet at http://pubs.acs.org.

■ AUTHOR INFORMATION

Corresponding Author
*E-mail: huiru.tang@wipm.ac.cn.

■ ACKNOWLEDGMENT

The authors acknowledge financial supports from National Basic Research Program of China (2010CB912501) and National Natural Science Foundation of China (20825520, 20903115, and 20921004). Jiming An at Center for Materials Research & Analysis of Wuhan University of Technology performed the DSC measurements as a paid service, and we thank Dr. Detlef Reichert at Physics Department of Halle University for providing the program for the DIPSHIFT simulation. Wuyang Liu and Lei Chen assisted in variable temperature NMR experiments.

■ REFERENCES

(1) Boutonnet-Fagegaltier, N.; Menegotto, J.; Lamure, A.; Duplaa, H.; Caron, A.; Lacabanne, C.; Bauer, M. *J. Pharm. Sci.* **2002**, *91* (6), 1548.
(2) Geppi, M.; Mollica, G.; Borsacchi, S.; Veracini, C. A. *Appl. Spectrosc. Rev.* **2008**, *43* (3), 202.
(3) Hong, M.; Gross, J. D.; Griffin, R. G. *J. Phys. Chem. B* **1997**, *101* (30), 5869.
(4) Schmidt-Rohr, K.; Kulik, A. S.; Beckham, H. W.; Ohlemacher, A.; Pawelzik, U.; Boeffel, C.; Spiess, H. W. *Macromolecules* **1994**, *27* (17), 4733.
(5) deAzevedo, E. R.; Hu, W. G.; Bonagamba, T. J.; Schmidt-Rohr, K. *J. Am. Chem. Soc.* **1999**, *121* (36), 8411.
(6) Andrew, E. R.; Hinshaw, W. S.; Hutchins, M. G.; Sjöblom, R. O. I. *Mol. Phys.* **1976**, *31* (5), 1479.
(7) Andrew, E. R.; Hinshaw, W. S.; Hutchins, M. G.; Sjöblom, R. O. I.; Canepa, P. C. *Mol. Phys.* **1976**, *32* (3), 795.
(8) Andrew, E. R.; Hinshaw, W. S.; Hutchins, M. G.; Sjöblom, R. O. I. *Mol. Phys.* **1977**, *34* (6), 1695.
(9) Krushelnitsky, A.; Zinkevich, T.; Mukhametshina, N.; Tarasova, N.; Gogolev, Y.; Gnezdilov, O.; Fedotov, V.; Belton, P.; Reichert, D. *J. Phys. Chem. B* **2009**, *113* (29), 10022.
(10) Tang, H. R.; Belton, P. S.; Ng, A.; Ryden, P. *J. Agric. Food Chem.* **1999**, *47* (2), 510.
(11) Tang, H. R.; Wang, Y. L.; Belton, P. S. *Solid State Nucl. Magn. Reson.* **2000**, *15* (4), 239.
(12) Tang, H. R.; Hills, B. P. *Biomacromolecules* **2003**, *4* (5), 1269.
(13) Wang, Y. L.; Tang, H. R.; Belton, P. S. *J. Phys. Chem. B* **2002**, *106* (49), 12834.
(14) Tang, H. R.; Wang, Y. L.; Belton, P. S. *Phys. Chem. Chem. Phys.* **2004**, *6* (13), 3694.
(15) Cai, W. Z.; Schmidt-Rohr, K.; Egger, N.; Gerharz, B.; Spiess, H. W. *Polymer* **1993**, *34* (2), 267.
(16) Miyoshi, T.; Takegoshi, K.; Hikichi, K. *Polymer* **1997**, *38* (10), 2315.
(17) Zhang, L. M.; Tang, H. R.; Hou, G. J.; Shen, Y. D.; Deng, F. *Polymer* **2007**, *48* (10), 2928.
(18) Van der Heide, T.; Poolman, B. *J. Bacteriol.* **2000**, *182* (1), 203.
(19) Mendum, M. L.; Smith, L. T. *Appl. Environ. Microbiol.* **2002**, *68* (2), 813.
(20) Craig, S. A. S. *Am. J. Clin. Nutr.* **2004**, *80* (3), 539.
(21) Ueland, P. M. *J. Inherit. Metab. Dis.* **2011**, *34* (1), 3.
(22) Sreekumar, A.; Poisson, L. M.; Rajendiran, T. M.; Khan, A. P.; Cao, Q.; Yu, J. D.; Laxman, B.; Mehra, R.; Lonigro, R. J.; Li, Y.; Nyati, M. K.; Ahsan, A.; Kalyana-Sundaram, S.; Han, B.; Cao, X. H.; Byun, J.; Omenn, G. S.; Ghosh, D.; Pennathur, S.; Alexander, D. C.; Berger, A.; Shuster, J. R.; Wei, J. T.; Varambally, S.; Beecher, C.; Chinnaiyan, A. M. *Nature* **2009**, *457* (7231), 910.
(23) Stephan, C.; Jentzmik, F.; Jung, K. *Eur. Urol.* **2010**, *58* (1), 20.
(24) Mostad, A.; Natarajan, S. *Acta Chem. Scand.* **1989**, *43* (10), 1004.
(25) Gómez-Zavaglia, A.; Fausto, R. *Vib. Spectrosc.* **2003**, *33* (1−2), 105.
(26) Engelke, F.; Michel, D.; Pille, F. *Phys. Status Solidi B* **1984**, *125* (2), 483.
(27) Gómez-Zavaglia, A.; Reva, I. D.; Fausto, R. *Phys. Chem. Chem. Phys.* **2003**, *5* (1), 41.

(28) Viertorinne, M.; Valkonen, J.; Pitkänen, I.; Mathlouthi, M.; Nurmi, J. *J. Mol. Struct.* **1999**, *477* (1−3), 23.
(29) Fischer, M. S.; Templeton, D. H.; Zalkin, A. *Acta Crystallogr. Sec. B* **1970**, *B 26* (OCT15), 1392.
(30) Yip, W. H.; Wang, R. J.; Mak, T. C. W. *Acta Crystallogr. Sec. C* **1990**, *46*, 717.
(31) Ramanuja, M. N.; Ramesh, K. P.; Ramakrishna, J. *Phys. Status Solidi B* **2006**, *243* (8), 1929.
(32) Machida, M.; Ikeda, H.; Kakiuchi, T.; Ishibashi, T.; Hasebe, K. *J. Phys. Soc. Jpn.* **2003**, *72* (9), 2250.
(33) Ramanuja, M. N.; Ramesh, K. P.; Ramakrishna, J. *Mol. Phys.* **2006**, *104* (20−21), 3213.
(34) Torchia, D. A. *J. Magn. Reson.* **1978**, *30* (3), 613.
(35) Vinogradov, E.; Madhu, P. K.; Vega, S. *Chem. Phys. Lett.* **1999**, *314* (5−6), 443.
(36) Webb, G. G.; Zilm, K. W. *J. Am. Chem. Soc.* **1989**, *111* (7), 2455.
(37) Herzfeld, J.; Berger, A. E. *J. Chem. Phys.* **1980**, *73* (12), 6021.
(38) Look, D. C.; Lowe, I. J. *J. Chem. Phys.* **1966**, *44* (8), 2995.
(39) Powles, J. G.; Mansfield, P. *Phys. Lett.* **1962**, *2* (2), 58.
(40) Powles, J. G.; Strange, J. H. *Proc. Phys. Soc.* **1963**, *82* (525), 6.
(41) Abragam, A. Oxford University Press: New York: 1961.
(42) Bielecki, A.; Burum, D. P. *J. Magn. Reson. Ser. A* **1995**, *116* (2), 215.
(43) Taylor, R. E.; Dybowski, C. *J. Mol. Struct.* **2008**, *889* (1−3), 376.
(44) Kameda, T.; Tamada, Y. *Int. J. Biol. Macromol.* **2009**, *44* (1), 64.
(45) Kubo, R.; Tomita, K. *J. Phys. Soc. Jpn.* **1954**, *9* (6), 888.
(46) Tang, H. R.; Belton, P. S. *Solid State Nucl. Magn. Reson.* **1998**, *12* (1), 21.
(47) Dunn, M. B.; McDowell, C. A. *Mol. Phys.* **1972**, *24* (5), 969.
(48) Andrew, E. R.; Jurga, K.; Szczesniak, E. *Mol. Phys.* **1988**, *65* (6), 1421.
(49) Albert, S.; Gutowsky, H. S.; Ripmeester, J. A. *J. Chem. Phys.* **1972**, *56* (7), 3672.
(50) McDowell, C. A.; Raghunathan, P.; Williams, D. S. *J. Chem. Phys.* **1977**, *66* (7), 3240.
(51) Ramanuja, M. N.; Ramesh, K. P.; Ramakrishna, J. *Mol. Phys.* **2009**, *107* (7), 643.
(52) Świergiel, J.; Piślewski, N.; Medycki, W.; Holderna-Natkaniec, K.; Milia, F. *Appl. Magn. Reson.* **2004**, *26* (3), 357.
(53) Tang, H. R.; Belton, P. S. *Solid State Nucl. Magn. Reson.* **2002**, *21* (3−4), 117.
(54) McCall, D. W.; Douglass, D. C. *Appl. Phys. Lett.* **1965**, *7* (1), 12.
(55) Ilczyszyn, M.; Godzisz, D.; Ilczyszyn, M. M.; Mierzwicki, K. *Chem. Phys.* **2006**, *323* (2−3), 231.
(56) Ye, C. H.; Fu, R. Q.; Hu, J. Z.; Hou, L.; Ding, S. W. *Magn. Reson. Chem.* **1993**, *31* (8), 699.
(57) Ren, P. P.; Reichert, D.; He, Q. H.; Zhang, L. M.; Tang, H. R. *J. Phys. Chem. B* **2011**, *115*, 2814.
(58) Haberkorn, R. A.; Stark, R. E.; van Willigen, H.; Griffin, R. G. *J. Am. Chem. Soc.* **1981**, *103* (10), 2534.